Electronic Supplementary Information (ESI)

Superaerophobic Hydrogels for Diaphragm Modification to Suppress Gas Crossover in Alkaline Water Electrolyzers

Soi Lee,[a,b] Jinseo Lee,[a,b] Seunghyun Lee,[a] Hyeongoo Kim,[a,b] Yunseok Kang,[a,b] Dong Woog Lee[a] and Jungki Ryu[a,b,c,d]*

[a]School of Energy and Chemical Engineering, Ulsan National Institute of Science and Technology (UNIST), Ulsan 44919, Republic of Korea. Email: jryu@unist.ac.kr

[b]Emergent Hydrogen Technology R&D Center, Ulsan National Institute of Science and Technology (UNIST), Ulsan 44919, Republic of Korea

[c]Graduate School of Carbon Neutrality, Ulsan National Institute of Science and Technology (UNIST), Ulsan 44919, Republic of Korea

[d]Center for Renewable Carbon, Ulsan National Institute of Science and Technology (UNIST) Ulsan 44919, Republic of Korea

Keywords: alkaline water electrolyzers, diaphragm, gas crossover, hydrogels, superaerophobicity, wettability

Table S1. Advantages and limitations of recently reported diaphragms for alkaline water electrolysis (AWE).

Ref	Separator	Advantage	Limitation	Gas crossover evaluation method
This study	PVA hydrogel-coated diaphragm	- Simple and scalable dip-coating method. - Effective gas crossover suppression while maintaining electrolysis performance and durability - Direct gas crossover validation under practical AWE operating conditions	- Optimization of coating thickness/loading required to balance ionic resistance and bubble detachment behavior	- Direct gas crossover measurement under practical cell operating conditions (GC) - Dissolved gas crossover evaluation via ORR-current analysis and direct DO quantification - Indirect evaluations (BPP and contact angle measurements)
S1	BILP- PE	- Excellent mechanical and chemical stability under strong alkaline conditions (30 wt% KOH)	- Complicated synthesis protocol	- HOR-based evaluation; no measurements under practical cell operating conditions
S2	Chitosan-doped composite diaphragm	- Derived from renewable natural biomass, offering sustainability	- Poor stability under strongly alkaline conditions	- No direct gas crossover data under practical AWE operating conditions; only indirect evaluations (e.g., BPP or contact angle measurements)
S3	POBP/ZrO_2	- Stable operation for over 900 h at 0.5 A cm^{-2}	- Long synthesis time (>32 h)	- No direct gas crossover data under practical AWE operating conditions; only indirect evaluations (e.g., BPP or contact angle measurements)
S4	Alkanolamine-functionalized zirconia-blended	- Very low area resistance (0.12 $\Omega \cdot cm^2$ in 30 wt% KOH at room temperature)	- Potential health hazards associated with alkanolamines	- Gas crossover was not evaluated
S5	Skeleton-supported organic/inorganic composite membrane	- Simple synthesis	- Limited applicability to other separator systems	- Direct gas crossover measurement under practical cell operating conditions (GC)
S6	Cellulose nanocrystals (CNC)-blended ZrO_2/polysulfone membrane	- High durability: 600 mA cm^{-2} at 2 V for 300 h in 10 wt% KOH	- High material cost due to cellulose nanocrystals	- H_2 permeation measured under applied differential pressure; no data under practical cell operating conditions

*Abbreviation: Benzimidazole-linked polymer (BiLP); Polyethylene (PE); Poly(oxindole biphenylene) (POBP); Cellulose nanocrystals (CNC)

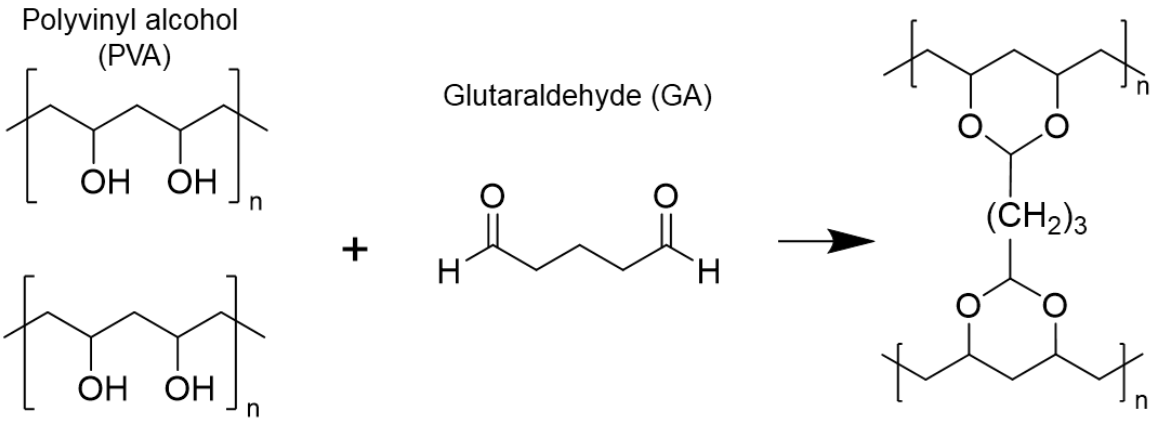

Fig. S1 Schematic illustration of the cross-linking reaction between PVA and glutaraldehyde, forming stable acetal linkages that generate three-dimensional hydrogel networks.

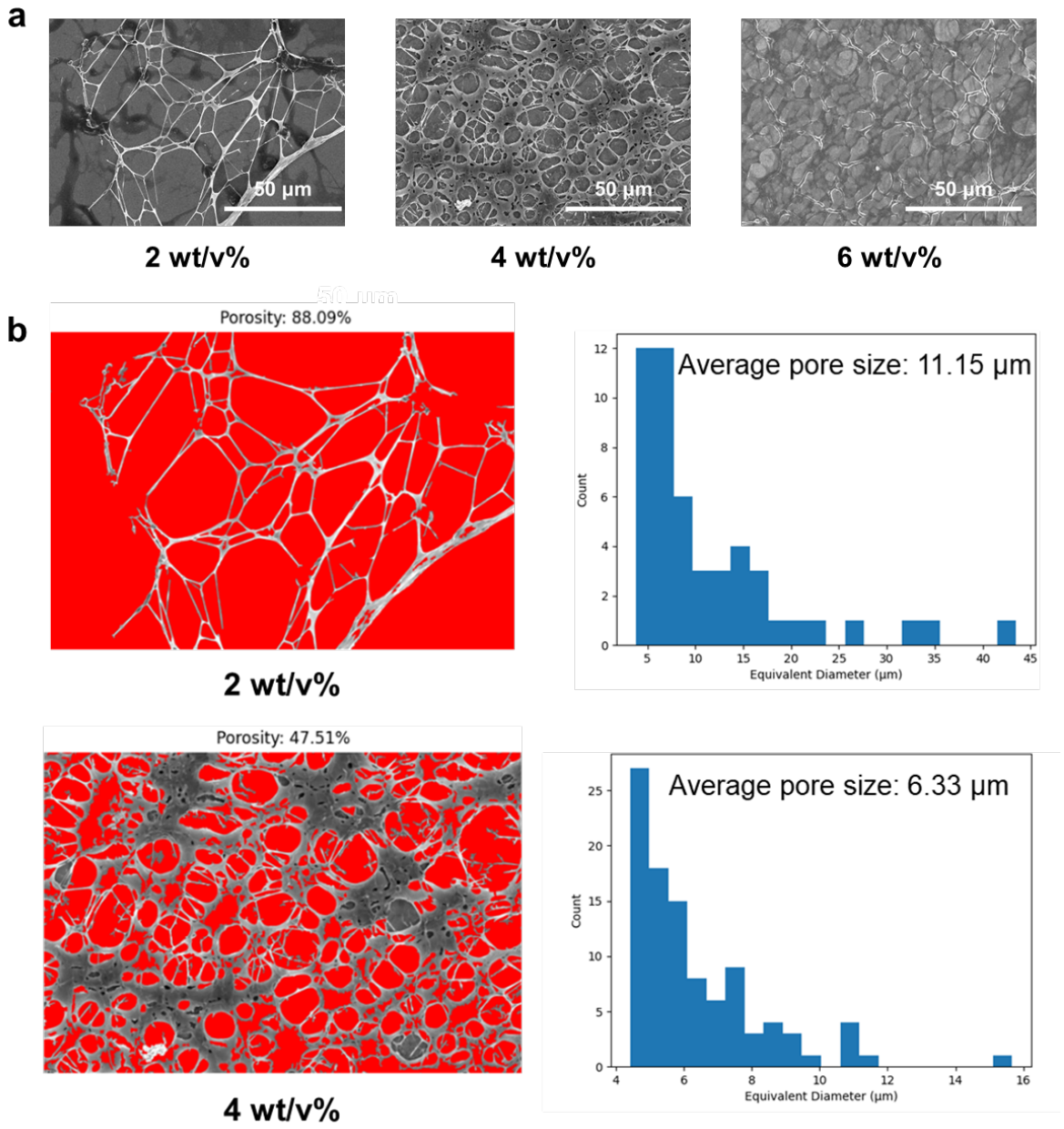

Fig. S2 Morphology and porosity analysis of PVA hydrogels on ITO substrates. (a) SEM images of PVA hydrogels with different concentrations coated on ITO substrates. (b) Calculated porosity and pore size distributions of 2 wt/v% and 4 wt/v% samples, showing average pore sizes of 11.15 µm and 6.33 µm, respectively.

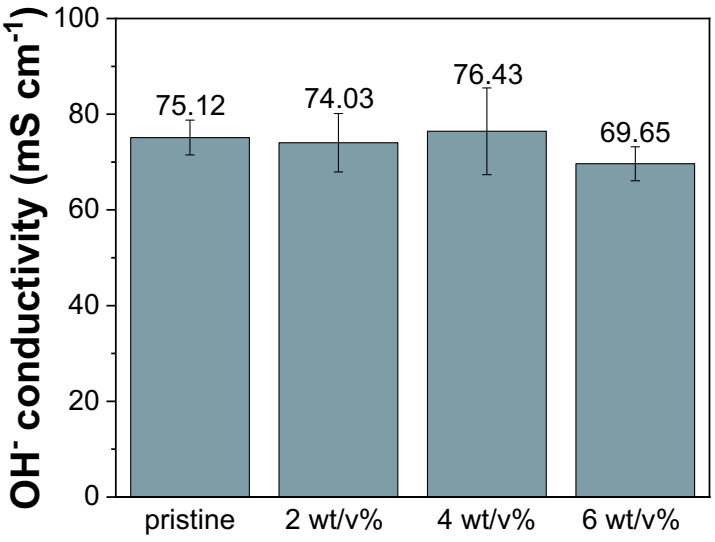

Fig. S3 OH^- conductivity of the pristine and PVA hydrogel-coated diaphragms. The OH^- conductivity of diaphragms remained nearly unchanged after hydrogel modification, except for the 6 wt/v% sample, which showed a slight decrease due to pore blockage.

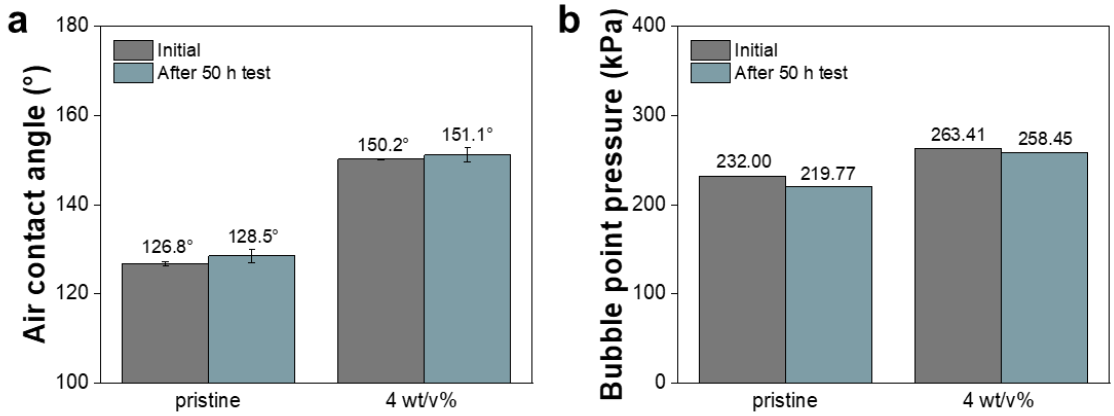

Fig. S4 (a) Air contact angles and (b) bubble point pressure (BPP) of the pristine diaphragm and the 4 wt/v% PVA hydrogel-coated diaphragm measured before and after 50 h immersion in 30 wt% KOH.

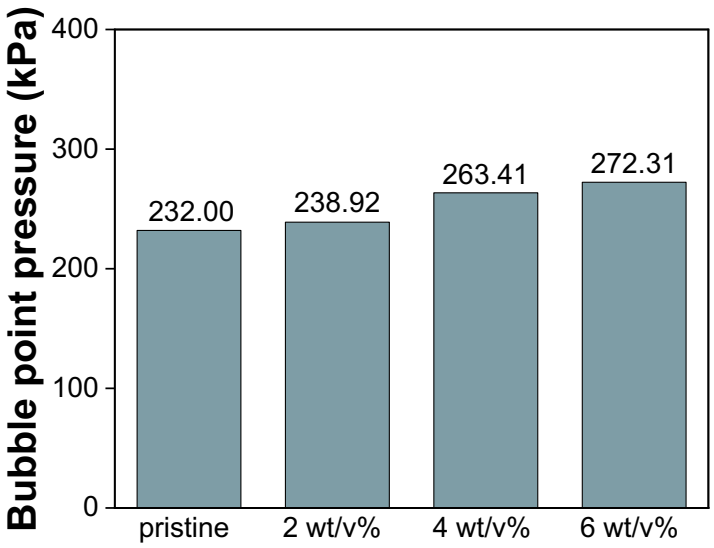

Fig. S5 Bubble point pressure of PVA hydrogel-coated diaphragms with different concentrations. Bubble point pressure (BPP) values increase with hydrogel modification, indicating enhanced resistance to gas permeation across the diaphragm.

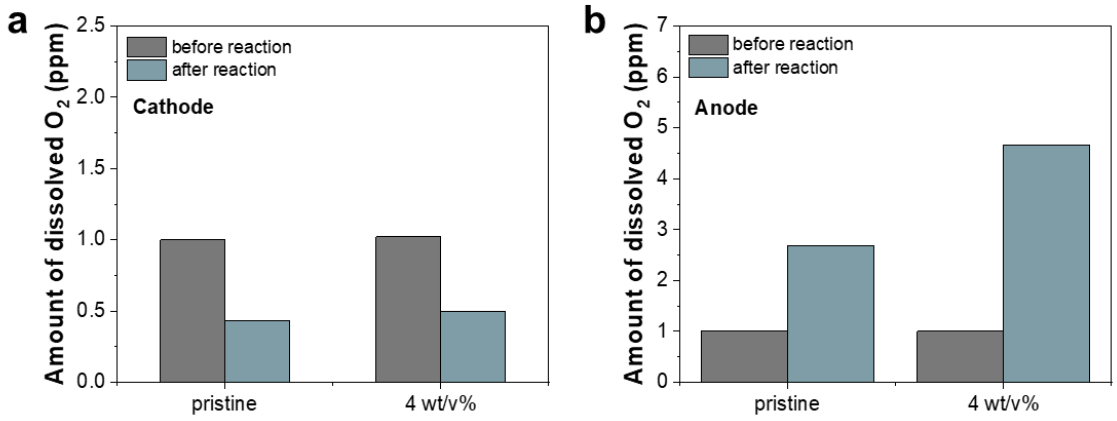

Fig. S6 Dissolved oxygen concentrations in the (a) cathode and (b) anode compartments before and after AWE operation at a low current density of 10 mA cm^{-2}.

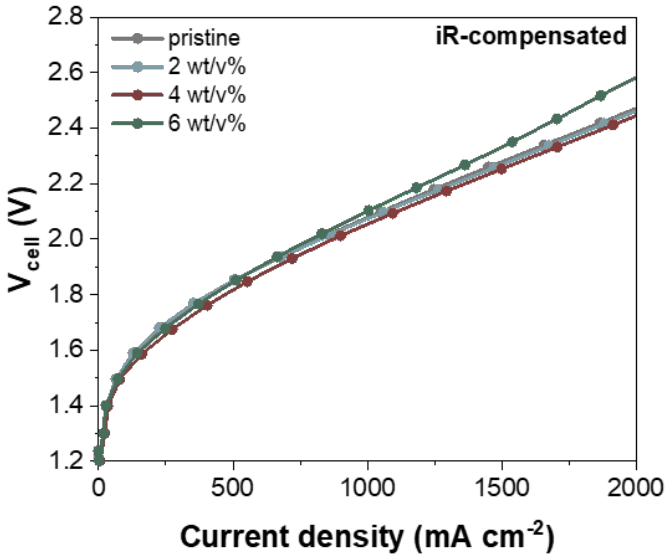

Fig. S7 iR-compensated polarization curves of pristine and hydrogel-coated diaphragms used in the AWE cell.

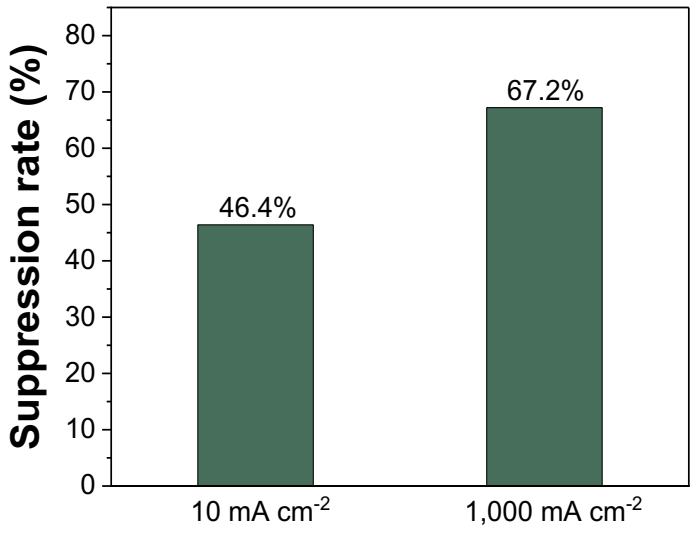

Fig. S8 Gas crossover suppression rate determined from GC measurements by comparing pristine and 4 wt/v% hydrogel-coated diaphragms after 2 h of operation.

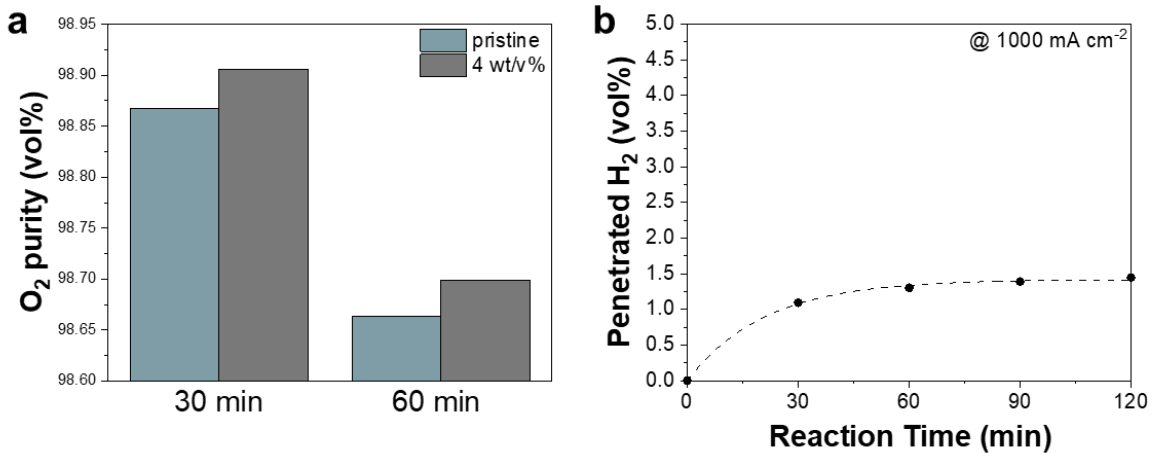

Fig. S9 Oxygen purity in the anode compartment of pristine and 4 wt/v% PVA hydrogel-coated AEMs. The hydrogel-coated AEM exhibited higher O_2 purity than the pristine membrane, confirming the effectiveness of superaerophobic surface modification in suppressing gas crossover.

Supporting References

S1. C. Song, L. Min, W. Zhang, L. Xu, Y. Wang, *J. Membrane Sci.* **2023**, *683*, 121883.

S2. J. Yu, Q. Zhu, W. Ma, Y. Dai, S. Zhang, F. Wang, H. Zhu, *ACS Appl. Mater. Interfaces* **2024**, *16*, 1394-1403.

S3. H. Li, M. Liu, B. Hu, X. Hu, M. He, J. Xin, C. Niu, Y. Huang, N. Li, Z. Xu, Q, Zhang, *J. Membrane Sci.* **2024**, *700*, 122658.

S4. X. Yuan, T. Yan, Z. Liu, P. Kang, *ACS Sustain. Chem. Eng.* **2023**, *11*, 4269-4278.

S5. Y Liao, G. Deng, H. Wu, L. Ding, H. Wang, *Adv. Funct. Mater.* **2024**, *34*, 2309871.

S6. J. W. Lee, J. H. Lee, C. Lee, H.-S. Cho, M. Kim S.-K. Kim, J. H. Joo, W.-C. Cho, C.-H. Kim, *Chem. Eng. J.* **2022**, *428*, 131149.